Research on surface plasmon resonance Sensing of metal nano hollow elliptic cylinder

Dandan Zhu
Yanshan University

lixixn kang
Yanshan University

Kai Tong (✉ tongkai@ysu.edu.cn)
Yanshan University

Shancheng Yu
ningbo Instiute of Measurement and Testing

JinGuo Chai
Yanshan University

Zhengtai Wang
Yanshan University

LuLu Xu
Yanshan University

Yuxuan Ren
Yanshan University

Research Article

Additional Declarations: No competing interests reported.

Abstract

In this article, a new three-dimensional multi-layered nanoscale elliptical cylinder structure-based surface plasmon resonance sensor is designed, which utilizes the finite difference time domain method and FDTD simulation software for numerical simulation. The top of the structure is an elliptical cylinder array attached to a gold film with nanoholes. The middle layer is a dielectric layer, which can restrict the electromagnetic field. The bottom layer is an Au film and Si substrate. Surface plasmon resonance is excited by a vertically incident plane wave structure, and the incident electromagnetic wave is coupled to local surface plasmon through gold nanoscale elliptical cylinders. By adjusting the relevant structural parameters, the structure's resonance wavelength and resonance depth can be well adjusted. The optimized sensing structure has a smaller half-width than the traditional solid elliptical cylinder, higher sensitivity, and a larger quality factor. This structure can detect refractive indices in both gaseous and liquid environments, overcome the disadvantage of only being able to sense in a single environment, and provide a new approach for surface plasmon resonance sensing in biology and chemistry.

Introduction

Surface plasmon resonance (SPR) is an optical phenomenon [1] that is widely used in fields such as medical detection, food testing, and environmental monitoring. The effective regulation of localized surface plasmon resonance (LSPR) effects through the artificial design and preparation of metal nano-periodic arrays have been widely applied in fields such as optical communication and sensing, demonstrating advantages over traditional detection technologies [3]. Compared to traditional detection techniques, SPR sensors have the advantages of real-time biological detection, high refractive index sensitivity, and no need for labeled samples. With the continuous development of nanofabrication and manufacturing technology, metal nanostructures that can excite surface plasmon resonance phenomena [4] have been widely applied in surface plasmon resonance sensing. In recent years, there have been many studies on the sensing and performance characteristics of nanoparticle shapes, including spherical, disc-shaped or plate-shaped, rod-shaped, cubic, cylindrical structures, and so on. This article focuses on studying the cylindrical structure.

In 2016, Xu et al. proposed a simple method for preparing large-scale nanostructure arrays and studied the feasibility of using different diameters and periods of nanoarrays for refractive index sensing, which increased sensitivity by 60% and quality factor by 190% [5]. In 2018, Wang et al. designed a periodic gold nano-ring array structure and analyzed the influence of structural parameters on refractive index sensitivity. Finally, the structure was prepared and validated by laser holographic lithography technology, achieving a sensitivity of 577nm/RIU [6]. In 2019, Sioma Debela designed a surface plasmon resonance sensor for three layers of bimetallic nanoparticles in various geometric shapes. By changing the geometric shape, shell thickness, dielectric constant of the intermediate medium, thickness of the intermediate medium, and aspect ratio of the three layers of bimetallic nanoparticles, the surface plasmon resonance frequency can be tuned to the desired spectral range [7]. In 2020, Jialin Ji studied the

surface plasmon resonance of silver nanospheres on a silicon substrate gold film and achieved an adjustment of the absorption peak from 590 nm to 510 nm by increasing the thickness of the gold film [8]. The classic structure of metal-dielectric-metal (MDM) plasmon resonance is closely related to its surface morphology, metal particle size, and shape, the refractive index of the environment, and so on. The particle size, shape, and spacing of gold nanoparticles have a significant impact on the wavelength and intensity of surface plasmon resonance. In addition, the gold-dielectric-gold surface plasmon resonance is also affected by the medium. In 2021, Shengxi Jiao designed a three-layer periodic artificial metamaterial sensing structure composed of silver nanodisks, intermediate dielectric layers, and bottom silver reflectors. By optimizing the parameter structure, an absorption rate of 98.68% was achieved at a half-wave peak width of 3.5nm, and the refractive index sensitivity reached 542nm/RIU [9]. In 2022, Jiabao Jiang designed a surface plasmon resonance sensor based on the metal-dielectric-metal (MDM) structure, which is composed of AU gratings and Al2O3 gratings. The maximum sensitivity can reach 362nm/RIU [10].

Most of the above-mentioned SPR sensors can only conduct high-sensitivity detection in a single environment and lack strong adaptability to the environment. In response to this problem, this article proposes a new type of refractive index sensor based on a gold nano-hollow elliptical cylinder multilayer film structure that is based on the MDM classic structure. The proposed structure is simulated and calculated using the FDTD method, revealing that the surface plasmon resonance wavelength is extremely sensitive to the refractive index. Compared to traditional elliptical cylinder-induced surface plasmon resonance sensors and other classic MDM structure sensors, the proposed structure has higher sensitivity and quality factors. At the same time, the structure can be used in both gas and liquid environments, with maximum sensitivities of 602nm/RIU and 578nm/RIU achieved in gas and liquid environments, respectively. This sensor has great application value for use in a single environment.

Sensing Structure and Theoretical Methods

The designed composite structure is shown in Fig. 1, consisting of a three-dimensional structure with a top layer of gold nano hollow elliptical cylinder array capable of generating surface plasmon resonance phenomenon on its surface, a dielectric layer in the middle, and a bottom layer of Si substrate, forming a metal-dielectric-metal multilayer film. The entire array extends periodically in the X and Y directions, as shown in the figure. The height of the top gold film is denoted as t1, the thickness of the dielectric layer is denoted as d1, the thickness of the bottom gold film is denoted as t2, and the thickness of the Si substrate is denoted as d3. The height of the gold nano hollow elliptical cylinder and the hollow cavity is denoted as h, the short axis length of the elliptical cylinder is denoted as R1, the long axis length of the elliptical cylinder is denoted as R2, and the radius of the hollow cavity is denoted as R3.

Analysis was performed using the three-dimensional finite-difference time-domain (FDTD) method and simulation software. This method is widely used in optical simulation and can obtain the reflection spectrum and field strength of composite material structures. Perfectly matched layer (PML) boundary conditions were used on the upper and lower boundaries in the Z direction, and the incident light was a

vertically incident plane wave. According to the Drude model [11], metals contain a large number of free electrons, which are influenced by external electromagnetic fields, resulting in oscillations that form plasmons. Under different conditions, there are three different modes of this resonance: one is the plasmon oscillation that occurs inside the structure, the second is the surface plasmon mode that can propagate along the structure surface, and the third is the localized surface plasmon resonance that oscillates in standing wave form.

Under the excitation of an external electric field, longitudinal plasma oscillations are generated inside the metal. By introducing appropriate boundary conditions into the metal Maxwell equations, the expression for the oscillation frequency inside the metal can be obtained:

$$\omega_p^2 = \frac{ne^2}{\varepsilon_0 m}$$

where n is the degree of electron freedom in the metal, e is the electron charge, m is the electron mass, and ε is the dielectric constant of the metal in a vacuum. According to the Drude model, the dielectric constant of the metal is expressed as:

$$\varepsilon_\omega = 1 - \frac{\omega_p^2}{\omega(\omega + i\omega_c)}$$

where the plasma frequency $\omega_p = 2\pi \times 2.175 \times 10^{15} Hz$, and metal scattering frequency $\omega_c = 2\pi \times 6.49 \times 10^{14} Hz$ [12], When incident light excites surface plasmon resonance in a composite structure, surface plasma waves become highly sensitive to changes in the environmental medium. Therefore, the deviation of the resonance wavelength corresponds to the refractive index (RI) change of the object to be measured. RI sensing can be achieved by establishing a curve corresponding to the RI of the object to be measured and the resonance wavelength. Refractive index sensitivity and figure of merit (FOM) are important indicators of sensor performance, and their values increase with better sensor performance. The refractive index sensitivity can be expressed as: $S = \frac{\Delta\lambda}{\Delta n}$, and the FOM can be expressed as: $FOM = \frac{S}{FWHM}$, where FWHM is the full-width at half-maximum of the plasmon resonance peak, and the smaller the FWHM, the higher the quality factor.

Discussion and analysis

Numerical simulations of the sensor were conducted using 3D FDTD method, where the corresponding structural parameters were set as h = 40nm, R1 = 100nm, R2 = 175nm, t1 = 50nm, d1 = 60nm, t2 = 200nm, and d2 = 2000nm. Figure 2(a) shows the reflectance spectrum of plasmonic resonance, where the energy of the incident light wave resonates with the surface plasmon wave, resulting in a resonance peak in the spectrum. The corresponding incident wavelength is the resonance wavelength, which can be found to be at 762nm. The resonance depth is the difference between the maximum reflectance and the peak reflectance, and it can also be represented as the coupling efficiency between the incident light and the metal surface plasmon wave. The deeper the depth, the greater the coupling efficiency. When the depth

reaches half of the corresponding wavelength, the width of the spectrum is the half-maximum width (FWHM). FWHM represents the loss degree of the surface plasmon polariton, where a wider FWHM leads to greater loss and poorer sensing performance.

Figure 2(b) shows the surface electric field distribution of the gold nanostructure at the plasmonic resonance peak of 765nm. The surface electric field distribution after plasmonic resonance can be seen more clearly in the figure. When light is irradiated onto the metal surface, there are many electrons on the surface of the metal, which collectively resonate with the light wave, resulting in a large amount of energy accumulation, numerically represented by the strength of the electric field. As shown in the figure, the electric field strength on both sides of the hollow elliptical cylinder is larger, while that at the hollow position is smaller, indicating that resonance occurs at the interface between the metal and the dielectric. The electric fields on both sides of the metal are highly concentrated, indicating that the plasmonic resonance is stronger in this area due to the sharper edges of the elliptical cylinder, which can accumulate a large number of electrons. At the same time, it can also be found that the electric field strength is larger on the surface of the hollow elliptical cylinder and smaller inside, which can fully prove that the plasmonic resonance occurs on the metal surface. The structural parameters will affect the performance of the plasmonic resonance sensor. To obtain the optimal performance of the sensor, it is necessary to optimize and analyze the structural parameters of the sensor. The parameters of the sensing structure mainly include the height of the gold nanocylinder, the ratio of its major and minor axes, the size of the hollow region, the period size, and the thickness of the dielectric layer.

Figure 3 shows the variation of the reflectance spectrum with the height of the gold nano hollow elliptical cylinder in the wavelength range of 700-900nm through FDTD simulations. When the height of the top AU hollow elliptical cylinder changes from 30nm to 60nm, the reflectance spectrum undergoes a redshift, and the resonance depth gradually decreases, while the FWHM slightly increases. When the height is 30nm, the resonance depth reaches 99.9%, the coupling efficiency is the highest, the reflectance is the largest, and the resonance effect is optimal.

For a cylinder, the main resonance mode is the transverse electromagnetic wave, and its resonance frequency is related to the height of the cylinder. When the height of the cylinder is small, the resonance frequency is high, while when the height of the cylinder is large, the resonance frequency is low. Therefore, the height of the cylinder affects the resonance mode. At the same time, the height of the cylinder also affects the local electric field strength and energy transfer efficiency of plasma resonance. When the height of the cylinder is within a certain range, the electric field strength is stronger and the energy transfer efficiency is higher, which leads to a stronger plasma resonance. When the height of the cylinder exceeds a threshold, the energy transfer efficiency decreases, resulting in a weakening of the plasma resonance intensity.

The length of the major and minor axes of the elliptical cylinder is also an important parameter that affects the sensor performance. When the length of the major and minor axes are 290nm and 200nm respectively, i.e., the ratio of the length of the major axis to that of the minor axis is 1.45:1, as shown in

Fig. 5, the resonance peak is at 757nm. With the increasing ratio of the length of the major axis to that of the minor axis, the resonance peak continuously shifts towards longer wavelengths, and the resonance depth gradually increases. When the ratio of the length of the major axis to that of the minor axis is 1.75:1, the resonance depth reaches over 99% at 767nm, achieving the best resonance effect. The ratio of the length of the major axis to that of the minor axis affects the effect of surface plasmon resonance and plays a crucial role in the performance of the sensor. When the ratio of the length of the major axis to that of the minor axis is larger, the ends become sharper and a large number of electrons gather at the edges, and the localized near-field characteristic of the metal nanostructure becomes more obvious. The more concentrated the free electrons are, the greater and more concentrated the energy generated by the free electron resonance will be. The excitation effect of this elliptical cylinder structure is significantly higher than the resonance strength of the cylinder, which provides a new idea for exciting plasma resonance in the cylinder.

Figure 5 shows the influence of the size of the hollow elliptical cylinder aperture on the resonance depth of the sensing structure. The reflection spectrum changes with the variation of the hollow aperture radius by simulation experiments. When the elliptical cylinder has no hole, its resonance depth is the smallest compared to that with a hole, indicating that the hollow structure affects the performance of the sensor.

When the aperture size increases, the spectrum shifts towards longer wavelengths, and the resonance depth increases accordingly. The maximum resonance depth is achieved when the aperture size is 40nm. The size of the hollow aperture directly affects the surface area of the excitation body, thereby affecting its resonance frequency and leading to changes in its coupling efficiency. When the elliptical cylinder has no hole, the surface area is small, and the resonance frequency is low; when there is a nanohole, the surface area of the excitation body increases, leading to an increase in resonance frequency and resonance depth, thereby improving the performance of the sensor. However, the resonance depth does not continue to increase when the aperture size reaches a threshold. Compared with the elliptical cylinder without a hole as the excitation body, the hollow elliptical cylinder has a higher coupling efficiency and superior sensing performance.

Periodicity is also an important parameter that affects the sensor performance. Figure 6 shows the variation of the reflection spectrum with the change of the period. As the period increases, the reflection spectrum shifts towards longer wavelengths. The resonance depths of the reflection spectra at 560nm, 580nm, 600nm, and 620nm all reach over 99%. For this structure, changing the period size can tune the resonance wavelength of the sensing structure.

In summary, the optimal geometric parameters of the composite material structure after parameter optimization are obtained. The height of the gold nano eccentric cylinder is 30nm, the length of its major axis is 175nm, the length of its minor axis is 100nm, the height of the top gold film is 40nm, the height of the dielectric layer is 50nm, the height of the bottom gold film is 60nm, and the height of the Si substrate is 2000nm, which is the optimal parameter. To further explore the sensor performance, the sensitivity of the sensor was analyzed. Refractive index sensing is achieved by measuring the shift of the resonant

peak position in the corresponding reflection spectrum with the change of refractive index. The larger the resonant peak shift per unit RI, the better the sensing performance and the higher the sensitivity. The figure below shows the reflection spectra of the sensor under different environmental refractive index changes in both liquid and gas conditions. It can be seen from the reflection spectra that as the refractive index of the measured object increases, the resonance wavelength shifts towards longer wavelengths, and the half-peak width and resonance depth of the spectrum are basically unaffected, so it can be used as a refractive index sensing device.

As shown in Fig. 7, the refractive index range of the measured gas is from 1.1 to 1.15. Changes in the environmental refractive index cause a shift in the resonance wavelength. Figure 8 shows the fitting curve of refractive index changes in the gas environment, and the sensitivity in the gas environment was calculated to be 602nm/RIU. As shown in Fig. 9, the refractive index range of the measured liquid is from 1.3 to 1.35, and the sensor sensitivity in the liquid environment was calculated to be 578nm/RIU. This structure is highly sensitive to refractive index changes in both gas and liquid environments. Compared with traditional elliptical cylinder nanostructure sensors with sensitivities of only a few tens, this structure has greatly improved sensitivity. The quality factor is also an important factor for measuring the performance of plasmon resonance sensors, represented by the ratio of sensitivity to FWHM. The quality factors in gas and liquid environments were calculated to be 78.1RIU-1 and 66.8RIU-1, respectively. Both the sensitivity and quality factors demonstrate that this sensing structure has superior performance and has great potential for applications in detecting small refractive index changes and as a tunable metal device. It also demonstrates high adaptability to gas and liquid environments, making it highly applicable for sensing in single-medium environments.

Conclusion

In conclusion, surface plasmon resonance has become a hot research area, and the AU-dielectric-AU nano-periodic array sensing structure designed based on this theoretical foundation has good stability. Simulating and optimizing its electromagnetic and spectral characteristics through finite difference methods can achieve high refractive index sensitivity detection in dual gas and liquid environments. Compared with traditional elliptical cylinder structures, it has higher sensitivity and quality factor in the visible light band, with a sensitivity of 578nm/RIU and 602nm/RIU in gas and liquid environments, respectively. The structure will provide new ideas for the wide application of surface plasmon resonance sensors in biochemistry sensing.

Declarations

The authors have no relevant financial or non-financial interests to disclose

Authors' contributions

Dandan Zhu[1],Lixin Kang[2],Kai Tong[3],Shancheng Yu[4]JinGuo Chai[5],Zhengtai Wang[6],LuLu Xu[7],Yuxuan Ren[8]

All authors contributed to the study of concept and design. All authors commented on previous versions of manuscripts. All authors read and approved the final manuscript.

Availability of data and materials

All data is available

References

1. Phillips, and K.S. Jirí Homola (Ed.), "Surface Plasmon Resonance Based Sensors," Anal Bioanal Chem **390**, 1221–1222 (2008).

2. Rapid Immunoglobulin M-Based Dengue Diagnostic Test Using Surface Plasmon Resonance Biosensor

3. Tu M H, Sun T, Grattan K T V. LSPR optical fibre sensors based on hollow gold nanostructures[J]. Sensors & Actuators B Chemical, 2014, 191(Feb.):37-44.

4. Yousefi M, Mozaffari N, Shirkani H. Modeling of near-infrared SPR sensors based on silver-graphene asymmetric grating and investigation of their capability of gases detection[J]. Physica, E. Low-dimensional systems & nanostructures, 2022(135-):135.

5. Xu X, Hu X, Chen X, et al. Engineering a Large Scale Indium Nanodot Array for Refractive Index Sensing[J]. ACS Applied Materials & Interfaces, 2016,8(46):31871-31877.

6. Wang S, Sun X, Ding M, et al. The investigation of an LSPR refractive index sensor based on periodic gold nanorings array[J]. Journal of physics. D, Applied physics, 2018,51(4):45101.

7. Debela S,Mesfin B, Senbeta T. Surface plasmon resonances in ellipsoidal bimetallic nanoparticles[J]. Photonics and Nanostructures-Fundamentals and Applications, 2019.4.

8. Ji J, Li Z, Sun W, et al. Surface plasmon resonance tuning in gold film on silver nanospheres through optical absorption[J]. Sensing and Bio-Sensing Research, 2020:100374.

9. Design of Infrared Plasma Absorber with High Refractive Index Sensitivity

10. Jiang J, Xu Y, Li Y, et al. Triple-band perfect absorber based on the gold-Al2O3-grating structure in visible and near-infrared wavelength range[J]. Optical and Quantum Electronics, 2022, 54(1):1-15.

11. Benavides-Cruz M, C Calderón-Ramón, Gomez-Aguilar J F, et al. Numerical simulation of metallic nanostructures interacting with electromagnetic fields using the Lorentz−Drude model and FDTD method[J]. International Journal of Modern Physics C, 2016:615393-357.

12. Yi Z, Liu M, Luo J, et al. Multiple surface plasmon resonances of square lattice nanohole arrays in Au-SiO2-Au multilayer films[J]. Optics Communications, 2017, 390:1-6.
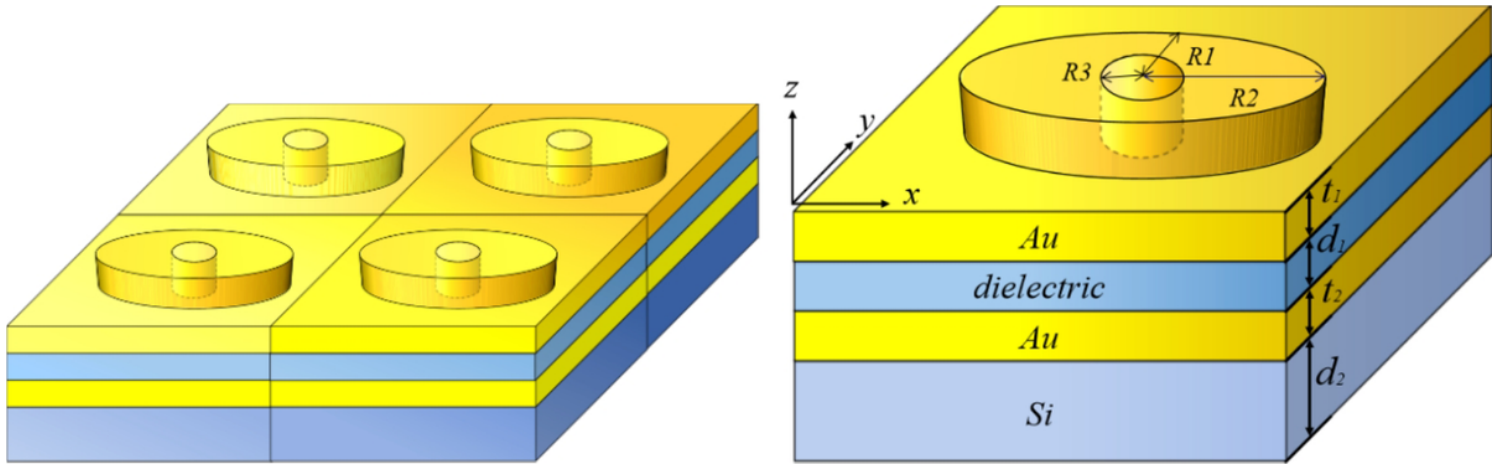
Figures

Figure 1

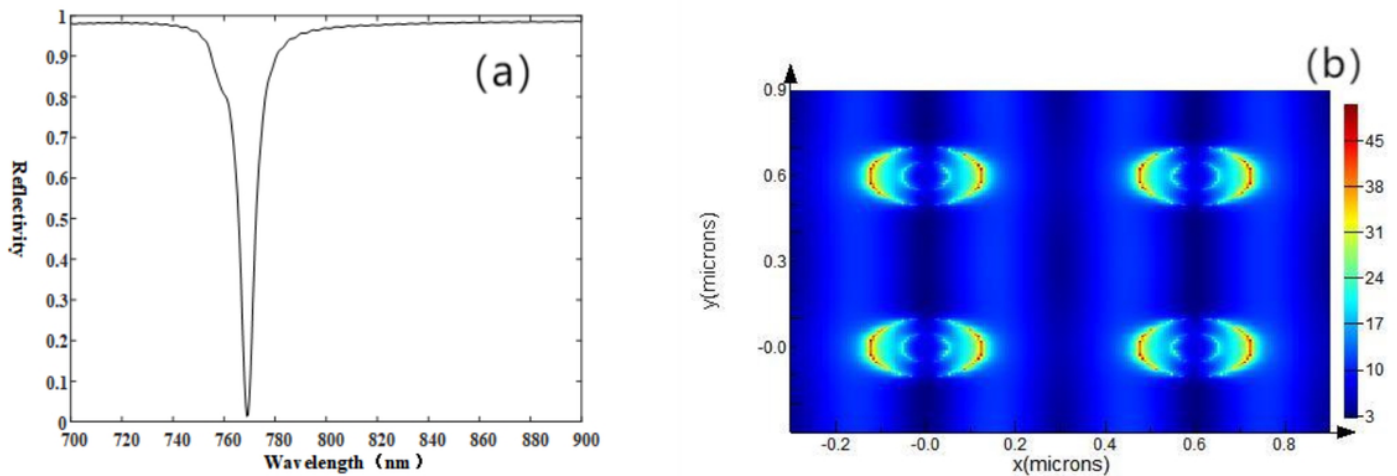Schematic diagram of the gold-dielectric-gold nano sensor structure

Figure 2

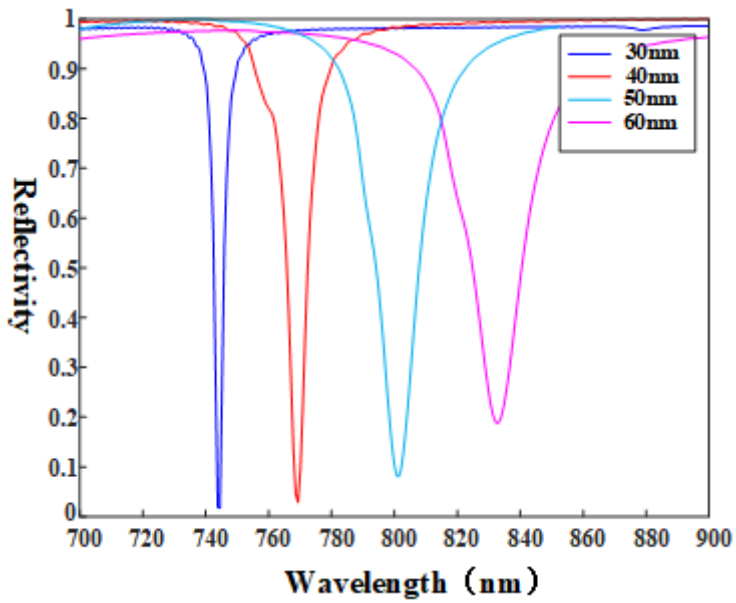Sensor performance   a Reflectance spectrum b Surface electric field

Figure 3

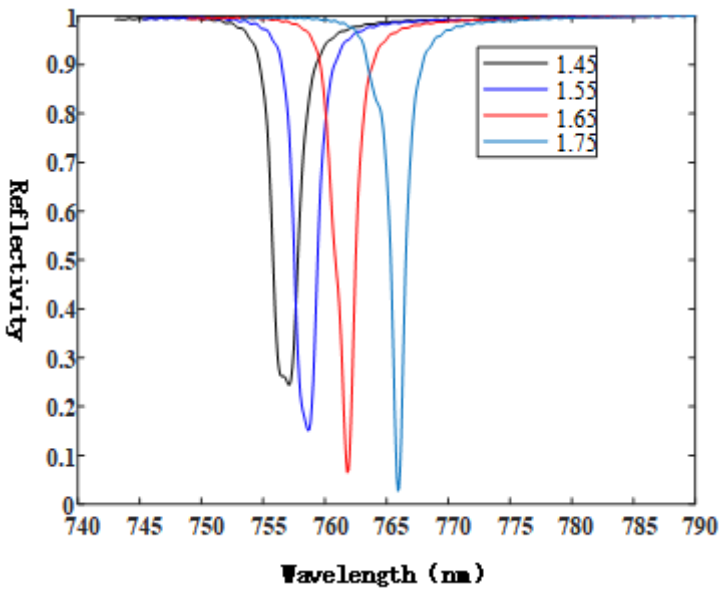Reflectance spectrum varies with height of elliptical cylinders

Figure 4

Variation of reflectance spectrum with the ratio of major and minor axes of elliptical cylinders
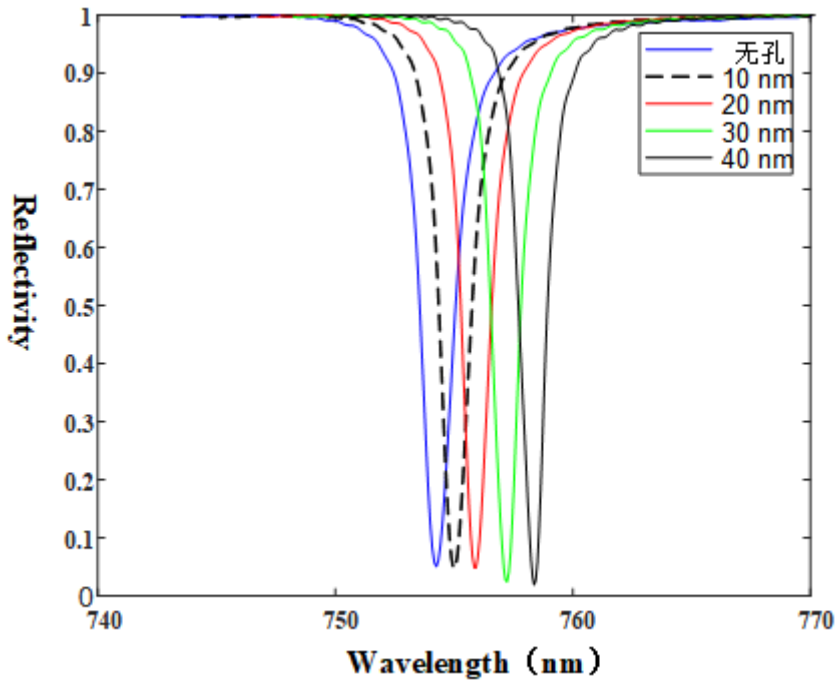
Figure 5

The reflectance spectrum varies with hollow aperture
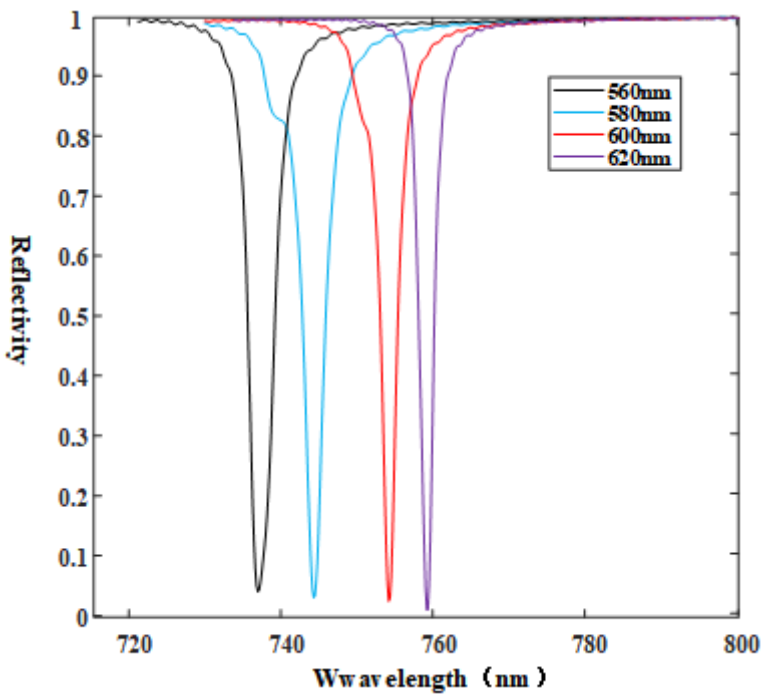
Figure 6

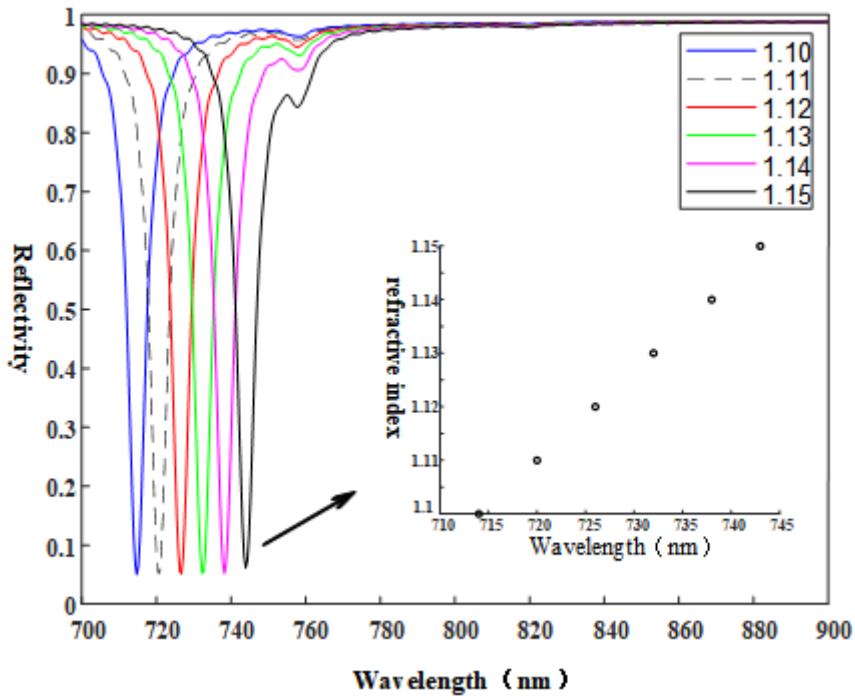Reflection spectrum of periodic changes in gold-electrolyte-gold structure

Figure 7

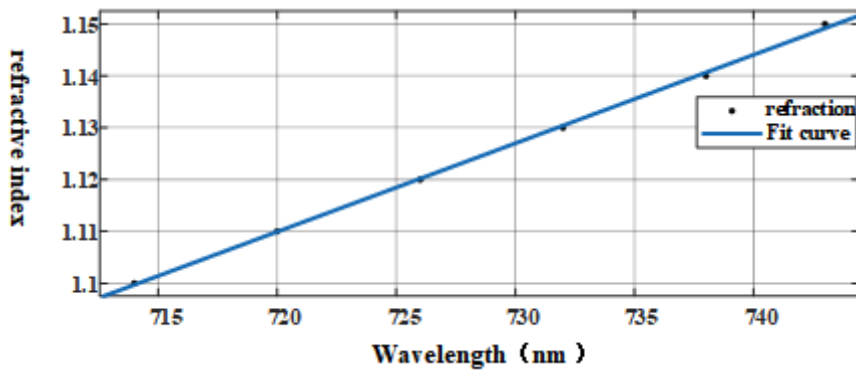Reflectance spectrum as a function of refractive index in a gas environment

Figure 8

Fitting curve of refractive index change in gas environment
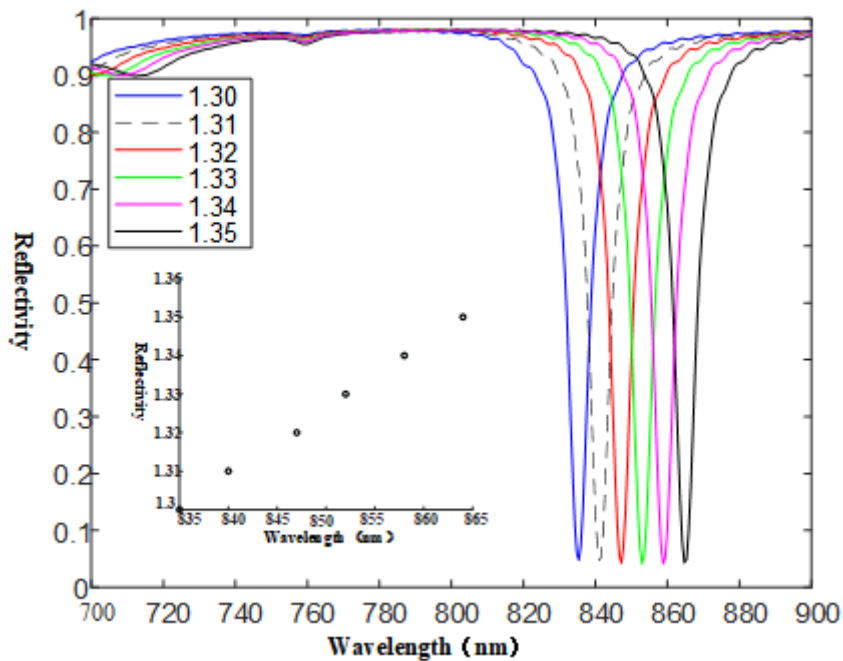
Figure 9

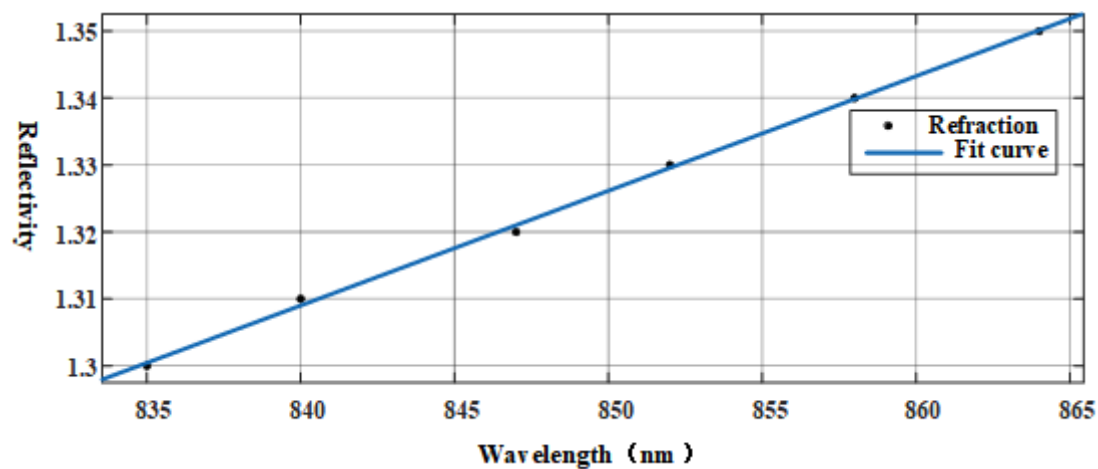Refractive index change reflectance spectrum in liquid environment

Figure 10

Fitting curve of environmental refractive index change in liquid environment